PERFORMANCE ANALYSIS OF ESPRIT-TYPE ALGORITHMS FOR STRICTLY NON-CIRCULAR SOURCES USING STRUCTURED LEAST SQUARES

Jens Steinwandt[1], *Florian Roemer*[2], *and Martin Haardt*[1]

[1] Communications Research Laboratory, Ilmenau University of Technology, P.O. Box 100565, 98684 Ilmenau, Germany
{jens.steinwandt, martin.haardt}@tu-ilmenau.de, www.tu-ilmenau.de/crl
[2] Digital Broadcasting Research Laboratory, Ilmenau University of Technology, P.O. Box 100565, 98684 Ilmenau, Germany
florian.roemer@tu-ilmenau.de

ABSTRACT

This paper presents a first-order analytical performance assessment of the 1-D non-circular (NC) Standard ESPRIT and the 1-D NC Unitary ESPRIT algorithms both using structured least squares (SLS) to solve the set of augmented shift invariance equations. These high-resolution parameter estimation algorithms were designed for strictly second-order (SO) non-circular sources and provide a reduced estimation error as well as an increased identifiability of twice as many sources. Our results are based on a first-order approximation of the estimation error that is explicit in the noise realizations and asymptotic in the effective signal-to-noise ratio (SNR), i.e., the approximation becomes exact for either high SNRs or a large sample size. We also find mean squared error (MSE) expressions, where only the assumptions of a zero mean and finite SO moments of the noise are required. Simulations show that the asymptotic performance of both algorithms is asymptotically identical in the high effective SNR.

***Index Terms*—** Performance analysis, Unitary ESPRIT, non-circular sources, structured least squares, DOA estimation.

1. INTRODUCTION

ESPRIT-type parameter estimation algorithms [1], [2] are some of the most prominent subspace-based high-resolution schemes and have gained a vast research interest. Due to their fully algebraic estimates and their low complexity, they are specifically attractive for a broad variety of applications such as radar, sonar, and wireless communications. With their increasing popularity, the importance of their analytical performance analyses has been stressed. The authors of [3] provide a first-order error approximation for 1-D Standard ESPRIT caused by the perturbed subspace estimate due to a small noise contribution, which is asymptotic in the effective signal-to-noise ratio (SNR), i.e., the result becomes exact for either high SNRs or a large sample size. This work was extended to R-D Unitary ESPRIT and R-D Standard/Unitary Tensor-ESPRIT in [4], where also the assumption of a circularly symmetric noise distribution for the mean squared error (MSE) in [3] was relaxed so that only a zero mean and finite second-order (SO) statistics of the noise are required. While [4] only considers least squares (LS) to solve the overdetermined set of shift invariance equations, its improved version, structured least squares (SLS) [5], has been integrated into the performance analysis presented in [6].

Recently, a number of improved parameter estimation schemes such as NC Standard ESPRIT [7] and NC Unitary ESPRIT [8] have been developed to exploit a priori knowledge about the source signals, i.e., their strict SO non-circularity. Examples include BPSK, ASK, and PAM-modulated signals. By applying a preprocessing procedure similar to the concept of widely-linear processing and thereby introducing additional degrees of freedom, the array aperture is virtually doubled. This results in a significantly reduced estimation error and the ability to detect twice as many sources. The analytical performance assessment of 1-D NC Standard ESPRIT and 1-D NC Unitary ESPRIT both using LS was presented in [9]. It was shown that NC Standard ESPRIT and NC Unitary ESPRIT have the same asymptotic performance in the high effective SNR and that NC Unitary ESPRIT does not require a centro-symmetric array structure unlike Unitary ESPRIT [2]. However, the performance analysis for the SLS solution of the augmented shift invariance equation has not been reported in the literature.

In this paper, we further extend the analytical performance assessment of 1-D NC Standard/Unitary ESPRIT using LS in [9] by incorporating one iteration of SLS [6] to solve the augmented shift invariance equation. We find the explicit first-order expansion for the estimation error in terms of the noise realization and generic MSE expressions, where we only assume that the noise has a zero mean and finite SO statistics, but no assumptions about the noise distribution are needed. Moreover, we show that in analogy to the LS case [9], the asymptotic performance of NC standard ESPRIT and NC Unitary ESPRIT both using SLS is asymptotically identical in the high effective SNR.

2. DATA MODEL FOR NC STRUCTURED LEAST SQUARES

We consider N subsequent snapshots of d narrowband signals in the far-field received by an arbitrarily formed shift-invariant M-element sensor array. The observations can be modeled as

$$\boldsymbol{X} = \boldsymbol{A}\boldsymbol{S} + \boldsymbol{N} \ \in \mathbb{C}^{M \times N}, \tag{1}$$

where $\boldsymbol{A} = [\boldsymbol{a}(\mu_1), \ldots, \boldsymbol{a}(\mu_d)] \in \mathbb{C}^{M \times d}$ is the array steering matrix that contains the d array steering vectors $\boldsymbol{a}(\mu_i)$ corresponding to the i-th spatial frequency with $i = 1, \ldots, d$, $\boldsymbol{S} \in \mathbb{C}^{d \times N}$ represents the source symbol matrix and $\boldsymbol{N} \in \mathbb{C}^{M \times N}$ models the additive noise samples. In the presumed case of strictly SO non-circular sources, the complex symbol amplitudes of each source form a rotated line in the complex plane so that $\boldsymbol{S}$ can be written as

$$\boldsymbol{S} = \boldsymbol{\Psi}\boldsymbol{S}_0, \tag{2}$$

This work was supported by the International Graduate School on Mobile Communications (MOBICOM), Ilmenau, Germany.

where $\boldsymbol{S}_0 \in \mathbb{R}^{d\times N}$ is a real-valued symbol matrix and $\boldsymbol{\Psi} = \mathrm{diag}\{e^{\mathrm{j}\varphi_i}\}_{i=1}^{d}$ contains complex phase shifts on its diagonal that can be different for each signal.

Applying a preprocessing procedure to (1) in order to exploit the sources' strict SO non-circularity, we define the augmented measurement matrix $\boldsymbol{X}^{(\mathrm{nc})}$ [8], [9] as

$$\boldsymbol{X}^{(\mathrm{nc})} = \begin{bmatrix}\boldsymbol{X}\\ \boldsymbol{\Pi}_M\boldsymbol{X}^*\end{bmatrix} = \begin{bmatrix}\boldsymbol{A}\\ \boldsymbol{\Pi}_M\boldsymbol{A}^*\boldsymbol{\Psi}^*\boldsymbol{\Psi}^*\end{bmatrix}\boldsymbol{S} + \begin{bmatrix}\boldsymbol{N}\\ \boldsymbol{\Pi}_M\boldsymbol{N}^*\end{bmatrix} \quad (3)$$

$$= \boldsymbol{A}^{(\mathrm{nc})}\boldsymbol{S} + \boldsymbol{N}^{(\mathrm{nc})} = \boldsymbol{X}_0^{(\mathrm{nc})} + \boldsymbol{N}^{(\mathrm{nc})} \in \mathbb{C}^{2M\times N}, \quad (4)$$

where $\boldsymbol{\Pi}_M \in \mathbb{R}^{M\times M}$ is the exchange matrix with ones on its antidiagonal and zeros elsewhere, used to facilitate the real-valued implementation of NC Unitary ESPRIT [8], and $\boldsymbol{X}_0^{(\mathrm{nc})} \in \mathbb{C}^{2M\times N}$ is the noise-free augmented measurement matrix. The extended dimensions of $\boldsymbol{A}^{(\mathrm{nc})} \in \mathbb{C}^{2M\times d}$ can be interpreted as a virtual doubling of the number of sensor elements, which also doubles the number of detectable sources and provides a lower estimation error. If the physical array is shift-invariant, $\boldsymbol{J}_1\boldsymbol{A}\boldsymbol{\Phi} = \boldsymbol{J}_2\boldsymbol{A}$ holds, where $\boldsymbol{J}_1$ and $\boldsymbol{J}_2 \in \mathbb{R}^{M^{(\mathrm{sel})}\times M}$ are the selection matrices for the two subarrays and $\boldsymbol{\Phi} = \mathrm{diag}\{[e^{\mathrm{j}\mu_1}, \ldots, e^{\mathrm{j}\mu_d}]\} \in \mathbb{C}^{d\times d}$ contains the desired spatial frequencies. It can be shown that in this case, the augmented array steering matrix $\boldsymbol{A}^{(\mathrm{nc})}$ is also shift-invariance-structured so that

$$\boldsymbol{J}_1^{(\mathrm{nc})}\boldsymbol{A}^{(\mathrm{nc})}\boldsymbol{\Phi} = \boldsymbol{J}_2^{(\mathrm{nc})}\boldsymbol{A}^{(\mathrm{nc})}, \quad (5)$$

where the $(2M^{(\mathrm{sel})}\times 2M)$-dimensional selection matrices in the NC case are defined by

$$\boldsymbol{J}_1^{(\mathrm{nc})} = \begin{bmatrix}\boldsymbol{J}_1 & \boldsymbol{0}\\ \boldsymbol{0} & \boldsymbol{\Pi}_{M^{(\mathrm{sel})}}\boldsymbol{J}_2\boldsymbol{\Pi}_M\end{bmatrix}, \boldsymbol{J}_2^{(\mathrm{nc})} = \begin{bmatrix}\boldsymbol{J}_2 & \boldsymbol{0}\\ \boldsymbol{0} & \boldsymbol{\Pi}_{M^{(\mathrm{sel})}}\boldsymbol{J}_1\boldsymbol{\Pi}_M\end{bmatrix}.$$

The augmented signal subspace $\hat{\boldsymbol{U}}_{\mathrm{s}}^{(\mathrm{nc})} \in \mathbb{C}^{2M\times d}$ is estimated by computing the d dominant left singular vectors of $\boldsymbol{X}^{(\mathrm{nc})}$. As $\boldsymbol{A}^{(\mathrm{nc})}$ and $\hat{\boldsymbol{U}}_{\mathrm{s}}^{(\mathrm{nc})}$ span approximately the same column space, a non-singular matrix $\boldsymbol{T} \in \mathbb{C}^{d\times d}$ can be found such that $\boldsymbol{A}^{(\mathrm{nc})} \approx \hat{\boldsymbol{U}}_{\mathrm{s}}^{(\mathrm{nc})}\boldsymbol{T}$. Then, the augmented shift invariance equation can be expressed as

$$\boldsymbol{J}_1^{(\mathrm{nc})}\hat{\boldsymbol{U}}_{\mathrm{s}}^{(\mathrm{nc})}\boldsymbol{\Upsilon} \approx \boldsymbol{J}_2^{(\mathrm{nc})}\hat{\boldsymbol{U}}_{\mathrm{s}}^{(\mathrm{nc})}, \quad (6)$$

where $\boldsymbol{\Upsilon} \approx \boldsymbol{T}\boldsymbol{\Phi}\boldsymbol{T}^{-1}$. Often, the unknown matrix $\boldsymbol{\Upsilon}$ is estimated using the least squares (LS) solution, i.e.,

$$\hat{\boldsymbol{\Upsilon}}_{\mathrm{LS}} = \left(\boldsymbol{J}_1^{(\mathrm{nc})}\hat{\boldsymbol{U}}_{\mathrm{s}}^{(\mathrm{nc})}\right)^+ \boldsymbol{J}_2^{(\mathrm{nc})}\hat{\boldsymbol{U}}_{\mathrm{s}}^{(\mathrm{nc})} \in \mathbb{C}^{d\times d}, \quad (7)$$

where $(\cdot)^+$ stands for the Moore-Penrose pseudo inverse. Finally, the estimates of the desired spatial frequencies are extracted by $\hat{\mu}_i = \arg\{\mathrm{EV}_i\{\hat{\boldsymbol{\Upsilon}}_{\mathrm{LS}}\}\}$, where $\mathrm{EV}_i\{\hat{\boldsymbol{\Upsilon}}_{\mathrm{LS}}\}$ is the i-th eigenvalue of $\hat{\boldsymbol{\Upsilon}}_{\mathrm{LS}}$.

A more accurate estimate of $\boldsymbol{\Upsilon}$ than (7) can be obtained via the structured least squares (SLS) algorithm [5]. It improves the LS solution by allowing for errors on both sides of the augmented shift invariance equation, i.e., errors in $\hat{\boldsymbol{U}}_{\mathrm{s}}^{(\mathrm{nc})}$ and $\boldsymbol{\Upsilon}$, and additionally takes into account the dependency of these errors due to the subarray overlap. Specifically, SLS solves the minimization problem

$$\min_{\Delta\boldsymbol{\Upsilon},\Delta\boldsymbol{U}_{\mathrm{s,SLS}}^{(\mathrm{nc})}} \big\|\boldsymbol{J}_1^{(\mathrm{nc})}(\hat{\boldsymbol{U}}_{\mathrm{s}}^{(\mathrm{nc})} + \Delta\boldsymbol{U}_{\mathrm{s,SLS}}^{(\mathrm{nc})})(\hat{\boldsymbol{\Upsilon}}_{\mathrm{LS}} + \Delta\boldsymbol{\Upsilon}_{\mathrm{SLS}}) - \boldsymbol{J}_2^{(\mathrm{nc})}(\hat{\boldsymbol{U}}_{\mathrm{s}}^{(\mathrm{nc})} + \Delta\boldsymbol{U}_{\mathrm{s,SLS}}^{(\mathrm{nc})})\big\|_{\mathrm{F}}^2 + \kappa^2\big\|\Delta\boldsymbol{U}_{\mathrm{s,SLS}}^{(\mathrm{nc})}\big\|_{\mathrm{F}}^2, \quad (8)$$

where κ is the regularization factor. The problem (8) is quadratic and solved iteratively by successive local linearization. However, it is asymptotically linear such that the first iteration is already sufficient in the high effective SNR regime. Therefore, we also limit the presented asymptotic performance analysis to one iteration. Additionally, we set $\kappa = 0$, since no regularization is required in the high effective SNR regime.

3. PERFORMANCE OF NC STANDARD ESPRIT WITH SLS

It was shown in [9] that the first-order analytical framework developed in [3] is directly applicable to the preprocessed model (4) for 1-D NC Standard/Unitary ESPRIT, where the authors only considered LS to solve the set of augmented shift invariance equations. Inspired by the work in [6], we here extend the performance analysis of 1-D NC Standard ESPRIT [9] to the case of using SLS to solve the overdetermined set of augmented shift invariance equations. We find a first-order expression for the parameter estimation error and an MSE expression for the case when SLS is incorporated.

From [9], we know that the estimation error of the i-th spatial frequency obtained by the LS solution may be expressed as

$$\Delta\mu_i = \mathrm{Im}\left\{\boldsymbol{p}_i^T\Delta\boldsymbol{\Upsilon}_{\mathrm{LS}}\boldsymbol{q}_i\right\}/\lambda_i + \mathcal{O}\{\Delta^2\} \quad \text{with} \quad (9)$$

$$\Delta\boldsymbol{\Upsilon}_{\mathrm{LS}} = \left(\boldsymbol{J}_1^{(\mathrm{nc})}\boldsymbol{U}_{\mathrm{s}}^{(\mathrm{nc})}\right)^+\left(\boldsymbol{J}_2^{(\mathrm{nc})}\Delta\boldsymbol{U}_{\mathrm{s}}^{(\mathrm{nc})} - \boldsymbol{J}_1^{(\mathrm{nc})}\Delta\boldsymbol{U}_{\mathrm{s}}^{(\mathrm{nc})}\boldsymbol{\Upsilon}\right),$$

where $\Delta = \|\boldsymbol{N}^{(\mathrm{nc})}\|$ with $\|\cdot\|$ being a submultiplicative norm, $\boldsymbol{q}_i$ represents the i-th eigenvector of $\boldsymbol{\Upsilon}$, i.e, the i-th column vector of the eigenvector matrix $\boldsymbol{Q}$, and $\boldsymbol{p}_i^T$ is the i-th row vector of $\boldsymbol{P} = \boldsymbol{Q}^{-1}$. Hence, the eigendecomposition of $\boldsymbol{\Upsilon}$, which is the solution to (6) in the noiseless case, is given by

$$\boldsymbol{\Upsilon} = \boldsymbol{Q}\boldsymbol{\Lambda}\boldsymbol{Q}^{-1}, \quad (10)$$

where the diagonal matrix $\boldsymbol{\Lambda}$ contains the eigenvalues $\lambda_i = e^{j\mu_i}$ on its diagonal. The matrix $\Delta\boldsymbol{U}_{\mathrm{s}}^{(\mathrm{nc})}$ denotes the signal subspace estimation error according to $\hat{\boldsymbol{U}}_{\mathrm{s}}^{(\mathrm{nc})} = \boldsymbol{U}_{\mathrm{s}}^{(\mathrm{nc})} + \Delta\boldsymbol{U}_{\mathrm{s}}^{(\mathrm{nc})}$ and is given by the expression

$$\Delta\boldsymbol{U}_{\mathrm{s}}^{(\mathrm{nc})} = \boldsymbol{U}_{\mathrm{n}}^{(\mathrm{nc})}\boldsymbol{U}_{\mathrm{n}}^{(\mathrm{nc})^H}\boldsymbol{N}^{(\mathrm{nc})}\boldsymbol{V}_{\mathrm{s}}^{(\mathrm{nc})}\boldsymbol{\Sigma}_{\mathrm{s}}^{(\mathrm{nc})^{-1}} + \mathcal{O}\{\Delta^2\}. \quad (11)$$

The matrices $\boldsymbol{U}_{\mathrm{n}}^{(\mathrm{nc})} \in \mathbb{C}^{2M\times(2M-d)}$, $\boldsymbol{V}_{\mathrm{s}}^{(\mathrm{nc})} \in \mathbb{C}^{N\times d}$, and $\boldsymbol{\Sigma}_{\mathrm{s}}^{(\mathrm{nc})} \in \mathbb{C}^{d\times d}$ are extracted from the economy size SVD of the noise-free measurement matrix $\boldsymbol{X}_0^{(\mathrm{nc})}$, where the columns of $\boldsymbol{U}_{\mathrm{n}}^{(\mathrm{nc})}$ and $\boldsymbol{V}_{\mathrm{s}}^{(\mathrm{nc})}$ span the noise subspace and the row space respectively, and $\boldsymbol{\Sigma}_{\mathrm{s}}^{(\mathrm{nc})}$ is the diagonal matrix with the singular values on its diagonal. It should be noted that (11) is explicit in the noise term $\boldsymbol{N}^{(\mathrm{nc})}$ and thus, no assumptions about the statistics of $\boldsymbol{N}$ are required.

In order to incorporate SLS into the performance analysis, we only consider one iteration and set $\kappa = 0$ as discussed before. We expand (8) and apply the property $\mathrm{vec}\{\boldsymbol{A}\boldsymbol{X}\boldsymbol{B}\} = (\boldsymbol{B}^T \otimes \boldsymbol{A}) \cdot \mathrm{vec}\{\boldsymbol{X}\}$ for arbitrary matrices $\boldsymbol{A}$, $\boldsymbol{B}$, and $\boldsymbol{X}$ of appropriate sizes. Hence, (8) reduces to

$$\min_{\Delta\boldsymbol{v}_{\mathrm{SLS}},\,\Delta\boldsymbol{u}_{\mathrm{s,SLS}}^{(\mathrm{nc})}} \left\|\hat{\boldsymbol{r}}_{\mathrm{LS}}^{(\mathrm{nc})} + \hat{\boldsymbol{F}}_{\mathrm{SLS}}\left[\Delta\boldsymbol{v}_{\mathrm{SLS}}^T \quad \Delta\boldsymbol{u}_{\mathrm{s,SLS}}^{(\mathrm{nc})^T}\right]^T\right\|_2^2, \quad (12)$$

where $\Delta\boldsymbol{v}_{\mathrm{SLS}} = \mathrm{vec}\{\Delta\boldsymbol{\Upsilon}_{\mathrm{SLS}}\}$, $\Delta\boldsymbol{u}_{\mathrm{s,SLS}}^{(\mathrm{nc})} = \mathrm{vec}\{\Delta\boldsymbol{U}_{\mathrm{s,SLS}}^{(\mathrm{nc})}\}$, and the augmented residual vector $\hat{\boldsymbol{r}}_{\mathrm{LS}}^{(\mathrm{nc})}$ and the update matrix $\hat{\boldsymbol{F}}_{\mathrm{SLS}}$ are expressed as

$$\hat{\boldsymbol{r}}_{\mathrm{LS}}^{(\mathrm{nc})} = \mathrm{vec}\left\{\boldsymbol{J}_1^{(\mathrm{nc})}\hat{\boldsymbol{U}}_{\mathrm{s}}^{(\mathrm{nc})}\hat{\boldsymbol{\Upsilon}}_{\mathrm{LS}} - \boldsymbol{J}_2^{(\mathrm{nc})}\hat{\boldsymbol{U}}_{\mathrm{s}}^{(\mathrm{nc})}\right\} \quad \text{and}$$

$$\hat{\boldsymbol{F}}_{\mathrm{SLS}} = \left[\boldsymbol{I}_d \otimes \left(\boldsymbol{J}_1^{(\mathrm{nc})}\hat{\boldsymbol{U}}_{\mathrm{s}}^{(\mathrm{nc})}\right) \quad \left(\hat{\boldsymbol{\Upsilon}}_{\mathrm{LS}}^T \otimes \boldsymbol{J}_1^{(\mathrm{nc})}\right) - \left(\boldsymbol{I}_d \otimes \boldsymbol{J}_2^{(\mathrm{nc})}\right)\right].$$

The solution to (12) is

$$\left[\Delta \boldsymbol{v}_{\mathrm{SLS}}^T \quad \Delta \boldsymbol{u}_{\mathrm{s,SLS}}^{(\mathrm{nc})^T}\right]^T = -\hat{\boldsymbol{F}}_{\mathrm{SLS}}^{+} \hat{\boldsymbol{r}}_{\mathrm{LS}}^{(\mathrm{nc})}. \tag{13}$$

Next, to find a first order approximation for the desired term $\Delta \boldsymbol{v}_{\mathrm{SLS}}$ in (13), we need the expansions of $\hat{\boldsymbol{F}}_{\mathrm{SLS}}^{+}$ and $\boldsymbol{r}_{\mathrm{LS}}$. Hence, we introduce the error term $\hat{\boldsymbol{\Upsilon}}_{\mathrm{LS}} = \boldsymbol{\Upsilon} + \Delta\boldsymbol{\Upsilon}_{\mathrm{LS}}$, so that we obtain

$$\hat{\boldsymbol{F}}_{\mathrm{SLS}}^{+} = \boldsymbol{F}_{\mathrm{SLS}}^{+} + \mathcal{O}\{\Delta\} \text{ and} \tag{14}$$

$$\boldsymbol{r}_{\mathrm{LS}} = \boldsymbol{W}_{\mathrm{R,U}}^{(\mathrm{nc})} \Delta \boldsymbol{u}_{s}^{(\mathrm{nc})} + \mathcal{O}\{\Delta^2\}, \tag{15}$$

where

$$\boldsymbol{F}_{\mathrm{SLS}} = \left[\boldsymbol{I}_d \otimes \left(\boldsymbol{J}_1^{(\mathrm{nc})} \boldsymbol{U}_{\mathrm{s}}^{(\mathrm{nc})}\right) \quad \left(\boldsymbol{\Upsilon}^T \otimes \boldsymbol{J}_1^{(\mathrm{nc})}\right) - \left(\boldsymbol{I}_d \otimes \boldsymbol{J}_2^{(\mathrm{nc})}\right)\right]$$

and

$$\begin{aligned}\boldsymbol{W}_{\mathrm{R,U}}^{(\mathrm{nc})} = &\left(\boldsymbol{\Upsilon}^T \otimes \boldsymbol{J}_1^{(\mathrm{nc})}\right) + \boldsymbol{I}_d \otimes \Big(\boldsymbol{J}_1^{(\mathrm{nc})} \boldsymbol{U}_{\mathrm{s}}^{(\mathrm{nc})} \\ &\cdot \left(\boldsymbol{J}_1^{(\mathrm{nc})} \boldsymbol{U}_{\mathrm{s}}^{(\mathrm{nc})}\right)^{+} \boldsymbol{J}_2^{(\mathrm{nc})}\Big) - \boldsymbol{\Upsilon}^T \otimes \Big(\boldsymbol{J}_1^{(\mathrm{nc})} \boldsymbol{U}_{\mathrm{s}}^{(\mathrm{nc})} \\ &\cdot \left(\boldsymbol{J}_1^{(\mathrm{nc})} \boldsymbol{U}_{\mathrm{s}}^{(\mathrm{nc})}\right)^{+} \boldsymbol{J}_1^{(\mathrm{nc})}\Big) - \left(\boldsymbol{I}_d \otimes \boldsymbol{J}_2^{(\mathrm{nc})}\right).\end{aligned} \tag{16}$$

Inserting (14) and (15) into (13) and dropping the second block of $\boldsymbol{F}_{\mathrm{SLS}}^H$ contained in $\boldsymbol{F}_{\mathrm{SLS}}^{+} = \boldsymbol{F}_{\mathrm{SLS}}^H \left(\boldsymbol{F}_{\mathrm{SLS}} \boldsymbol{F}_{\mathrm{SLS}}^H\right)^{-1}$ to extract $\Delta \boldsymbol{v}_{\mathrm{SLS}}$ [6], we have

$$\begin{aligned}\Delta \boldsymbol{v}_{\mathrm{SLS}} = &-\left(\boldsymbol{I}_d \otimes \left(\boldsymbol{J}_1^{(\mathrm{nc})} \boldsymbol{U}_{\mathrm{s}}^{(\mathrm{nc})}\right)\right)^H \\ &\cdot \left(\boldsymbol{F}_{\mathrm{SLS}} \boldsymbol{F}_{\mathrm{SLS}}^H\right)^{-1} \boldsymbol{W}_{\mathrm{R,U}}^{(\mathrm{nc})} \Delta \boldsymbol{u}_{\mathrm{s}}^{(\mathrm{nc})}.\end{aligned} \tag{17}$$

Then, the accumulated error after performing the first iteration of SLS is

$$\hat{\boldsymbol{\Upsilon}}_{\mathrm{SLS}} - \boldsymbol{\Upsilon} = \Delta\boldsymbol{\Upsilon}_{\mathrm{LS}} + \Delta\boldsymbol{\Upsilon}_{\mathrm{SLS}}, \tag{18}$$

where $\Delta\boldsymbol{\Upsilon}_{\mathrm{LS}}$ was given in (9) and $\Delta\boldsymbol{\Upsilon}_{\mathrm{SLS}}$ is the unvectorized version of (17). Next, we modify (9) by inserting (18) to write the first-order error expansion of the i-th spatial frequency as

$$\Delta\mu_{i,\mathrm{SLS}} = \mathrm{Im}\left\{\boldsymbol{p}_i^T \left(\Delta\boldsymbol{\Upsilon}_{\mathrm{LS}} + \Delta\boldsymbol{\Upsilon}_{\mathrm{SLS}}\right) \boldsymbol{q}_i\right\} / \lambda_i + \mathcal{O}\{\Delta^2\}. \tag{19}$$

Finally, to compute the MSE expression for NC Standard ESPRIT with SLS, we extend the result for LS in [9]. In [9] the authors have shown that the preprocessing procedure (3) does not violate the required assumptions of a zero mean and finite SO moments of the noise in order for the MSE expressions in [4] to be applicable in the NC case. As the incorporation of SLS instead of using LS merely provides a more accurate solution to the augmented shift invariance equation, we derive the MSE expression for the i-th spatial frequency in the SLS case, inspired by [9], as

$$\begin{aligned}\mathbb{E}\left\{(\Delta\mu_{i,\mathrm{SLS}})^2\right\} = &\frac{1}{2}\Big(\boldsymbol{r}_{i,\mathrm{SLS}}^{(\mathrm{nc})^H} \boldsymbol{W}^{(\mathrm{nc})^*} \boldsymbol{R}_{\mathrm{nn}}^{(\mathrm{nc})^T} \boldsymbol{W}^{(\mathrm{nc})^T} \boldsymbol{r}_{i,\mathrm{SLS}}^{(\mathrm{nc})} \\ &-\mathrm{Re}\left\{\boldsymbol{r}_{i,\mathrm{SLS}}^{(\mathrm{nc})^T} \boldsymbol{W}^{(\mathrm{nc})} \boldsymbol{C}_{\mathrm{nn}}^{(\mathrm{nc})^T} \boldsymbol{W}^{(\mathrm{nc})^T} \boldsymbol{r}_{i,\mathrm{SLS}}^{(\mathrm{nc})}\right\}\Big) + \mathcal{O}\{\Delta^2\},\end{aligned} \tag{20}$$

where

$$\begin{aligned}\boldsymbol{r}_{i,\mathrm{SLS}}^{(\mathrm{nc})} = &\boldsymbol{q}_i \otimes \left(\left[\left(\boldsymbol{J}_1^{(\mathrm{nc})} \boldsymbol{U}_{\mathrm{s}}^{(\mathrm{nc})}\right)^{+} \left(\boldsymbol{J}_2^{(\mathrm{nc})}/\lambda_i - \boldsymbol{J}_1^{(\mathrm{nc})}\right)\right]^T \boldsymbol{p}_i\right) \\ &- \boldsymbol{W}_{\mathrm{R,U}}^{(\mathrm{nc})^T} \left(\boldsymbol{F}_{\mathrm{SLS}} \boldsymbol{F}_{\mathrm{SLS}}^H\right)^{-T} \boldsymbol{q}_i \otimes \left(\left(\boldsymbol{J}_1^{(\mathrm{nc})} \boldsymbol{U}_{\mathrm{s}}^{(\mathrm{nc})}\right)^{*} / \lambda_i \boldsymbol{p}_i\right)\end{aligned}$$

and

$$\boldsymbol{W}^{(\mathrm{nc})} = \left(\boldsymbol{\Sigma}_{\mathrm{s}}^{(\mathrm{nc})^{-1}} \boldsymbol{V}_{\mathrm{s}}^{(\mathrm{nc})^T}\right) \otimes \left(\boldsymbol{U}_{\mathrm{n}}^{(\mathrm{nc})} \boldsymbol{U}_{\mathrm{n}}^{(\mathrm{nc})^H}\right).$$

The expressions for the covariance matrix $\boldsymbol{R}_{\mathrm{nn}}^{(\mathrm{nc})}$ and the pseudo-covariance matrix $\boldsymbol{C}_{\mathrm{nn}}^{(\mathrm{nc})}$ of $\boldsymbol{n}^{(\mathrm{nc})} = \mathrm{vec}\{\boldsymbol{N}^{(\mathrm{nc})}\} \in \mathbb{C}^{2MN \times 1}$ required in (20) were derived in [9]. They are given by

$$\begin{aligned}\boldsymbol{R}_{\mathrm{nn}}^{(\mathrm{nc})} &= \mathbb{E}\left\{\boldsymbol{n}^{(\mathrm{nc})} \boldsymbol{n}^{(\mathrm{nc})^H}\right\} \in \mathbb{C}^{2MN \times 2MN} \\ &= \tilde{\boldsymbol{K}} \begin{bmatrix} \boldsymbol{R}_{\mathrm{nn}} & \boldsymbol{C}_{\mathrm{nn}}(\boldsymbol{I}_N \otimes \boldsymbol{\Pi}_M) \\ (\boldsymbol{I}_N \otimes \boldsymbol{\Pi}_M)\boldsymbol{C}_{\mathrm{nn}}^* & (\boldsymbol{I}_N \otimes \boldsymbol{\Pi}_M)\boldsymbol{R}_{\mathrm{nn}}^*(\boldsymbol{I}_N \otimes \boldsymbol{\Pi}_M) \end{bmatrix} \tilde{\boldsymbol{K}}^H\end{aligned} \tag{21}$$

and

$$\begin{aligned}\boldsymbol{C}_{\mathrm{nn}}^{(\mathrm{nc})} &= \mathbb{E}\left\{\boldsymbol{n}^{(\mathrm{nc})} \boldsymbol{n}^{(\mathrm{nc})^T}\right\} \in \mathbb{C}^{2MN \times 2MN} \\ &= \tilde{\boldsymbol{K}} \begin{bmatrix} \boldsymbol{C}_{\mathrm{nn}} & \boldsymbol{R}_{\mathrm{nn}}(\boldsymbol{I}_N \otimes \boldsymbol{\Pi}_M) \\ (\boldsymbol{I}_N \otimes \boldsymbol{\Pi}_M)\boldsymbol{R}_{\mathrm{nn}}^* & (\boldsymbol{I}_N \otimes \boldsymbol{\Pi}_M)\boldsymbol{C}_{\mathrm{nn}}^*(\boldsymbol{I}_N \otimes \boldsymbol{\Pi}_M) \end{bmatrix} \tilde{\boldsymbol{K}}^T,\end{aligned} \tag{22}$$

where $\tilde{\boldsymbol{K}} = \boldsymbol{K}_{2M,N}^T (\boldsymbol{I}_2 \otimes \boldsymbol{K}_{M,N})$ is of size $2MN \times 2MN$ with the $MN \times MN$ commutation matrix $\boldsymbol{K}_{M,N}$ being the matrix that satisfies [10]

$$\boldsymbol{K}_{M,N} \cdot \mathrm{vec}\{\boldsymbol{A}\} = \mathrm{vec}\{\boldsymbol{A}^T\} \tag{23}$$

for arbitrary matrices $\boldsymbol{A} \in \mathbb{C}^{M \times N}$. Thus, the SO statistics of $\boldsymbol{n}^{(\mathrm{nc})}$ in (21) and (22) can be expressed by means of the covariance matrix $\boldsymbol{R}_{\mathrm{nn}} = \mathbb{E}\{\boldsymbol{n}\boldsymbol{n}^H\}$ and the pseudo-covariance matrix $\boldsymbol{C}_{\mathrm{nn}} = \mathbb{E}\{\boldsymbol{n}\boldsymbol{n}^T\}$ of the physical noise $\boldsymbol{n} = \mathrm{vec}\{\boldsymbol{N}\} \in \mathbb{C}^{MN \times 1}$. Note that (21) and (22) simplify to $\boldsymbol{R}_{\mathrm{nn}}^{(\mathrm{nc})} = \sigma_{\mathrm{n}}^2 \boldsymbol{I}_{2MN}$ and $\boldsymbol{C}_{\mathrm{nn}}^{(\mathrm{nc})} = \sigma_{\mathrm{n}}^2 (\boldsymbol{I}_N \otimes \boldsymbol{\Pi}_{2M})$ in the special case of zero-mean white circularly symmetric noise with $\boldsymbol{R}_{\mathrm{nn}} = \sigma_{\mathrm{n}}^2 \boldsymbol{I}_{MN}$ and $\boldsymbol{C}_{\mathrm{nn}} = \boldsymbol{0}_{MN}$.

4. PERFORMANCE OF NC UNITARY ESPRIT WITH SLS

We have shown in [9] that NC Standard ESPRIT and NC Unitary ESPRIT both using LS have the same analytical performance in the high effective SNR. The additional features of NC Unitary ESPRIT are the incorporation of forward-backward averaging (FBA) and the transformation into the real-valued domain to reduce the computational complexity. It was shown that applying FBA to the augmented measurement matrix $\boldsymbol{X}^{(\mathrm{nc})}$ does not improve the signal subspace estimate and that the real-valued transformation has no effect on the estimation performance in the high effective SNR regime.

The same behavior of an asymptotically identical performance of NC Standard ESPRIT and NC Unitary ESPRIT holds true when SLS is applied instead of LS. This is due to the fact that using SLS to solve the augmented shift invariance equation only provides a more accurate solution. It can be proven that the NC signal subspace for NC Standard ESPRIT and NC Unitary ESPRIT is modified in the same way.

5. SIMULATION RESULTS

In this section, we provide simulation results for the presented performance analysis of 1-D NC Standard/Unitary ESPRIT using SLS to solve the augmented shift invariance equation. We compare the results found analytically with the empirical estimation errors obtained by averaging over Monte Carlo trials. We consider a uniform linear array (ULA) composed of $M = 10$ isotropic sensor elements with interelement spacing $\delta = \lambda/2$ and assume that d sources with unit power and symbols drawn from a real-valued Gaussian distribution impinge on the array. Furthermore, we assume white Gaussian circularly symmetric noise at the sensor elements with $\sigma_n^2 = 10^{(-\mathrm{SNR}/10)}$ as discussed at the end of Section 3. The curves show

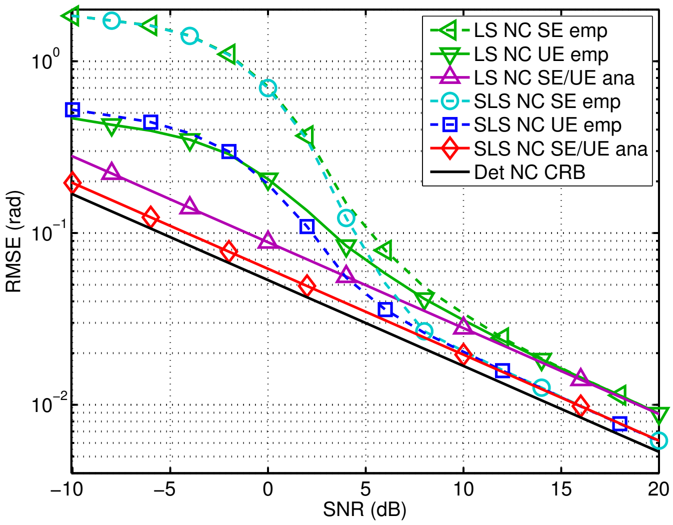

Fig. 1. Analytical and empirical RMSEs versus SNR for $M = 10$, $N = 20$, $d = 2$ correlated sources ($\rho = 0.9$) at $\mu_1 = -0.1$ and $\mu_2 = 0.1$ with rotation phases $\varphi_1 = 0$ and $\varphi_2 = \pi/4$.

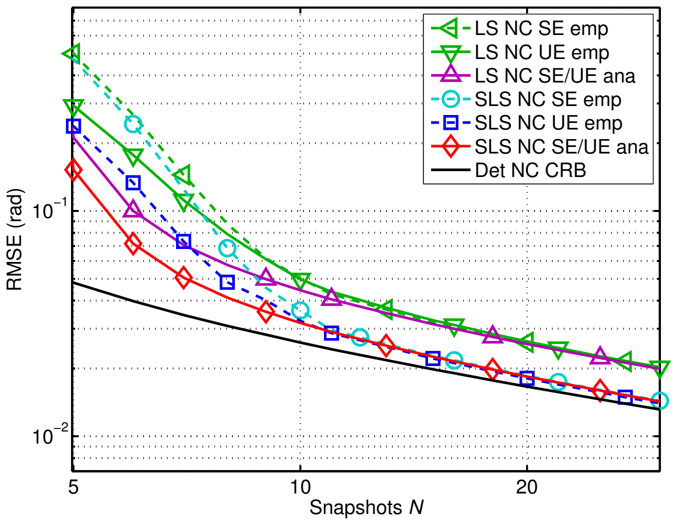

Fig. 2. Analytical and empirical RMSEs versus the snapshots N for $M = 10$, SNR $= 10$ dB, $d = 4$ sources at $\mu_1 = -0.5$, $\mu_2 = 0$, $\mu_3 = 0.5$, $\mu_4 = 1$ with rotation phases $\varphi_1 = 0$, $\varphi_2 = \pi/2$, $\varphi_3 = \pi/8$, $\varphi_4 = \pi/4$.

the total root mean squared error (RMSE) of the empirical simulations ("emp") for NC Standard ESPRIT with SLS (NC SE SLS), NC Unitary ESPRIT with SLS (NC UE SLS), and the square root of the analytical MSE expression (20) denoted as ("ana"). We also compare our results to their counterparts using LS and the deterministic NC Cramér-Rao bound [11]. The results are obtained by averaging over 5000 Monte Carlo trials.

In Fig. 1, we illustrate the RMSE as a function of the SNR. We assume $d = 2$ closely-spaced sources positioned at the spatial frequencies $\mu_1 = -0.1$ and $\mu_2 = 0.1$ with a pair-wise correlation of $\rho = 0.9$. The number of snapshots is $N = 20$ and the rotation phases contained in $\mathbf{\Psi}$ are given by $\varphi_1 = 0$ and $\varphi_2 = \pi/4$. It can be seen that the analytical results agree well with the empirical estimation errors for high SNRs. This also validates that the asymptotic performance of NC Standard ESPRIT and NC Unitary ESPRIT both using SLS is identical.

In Fig. 2, we display the RMSE versus the number of snapshots N. We have a scenario with $d = 4$ uncorrelated sources impinging from the directions $\mu_1 = -0.5$, $\mu_2 = 0$, $\mu_3 = 0.5$, $\mu_4 = 1$, where the SNR is chosen to be 10 dB. The rotation phases are given by $\varphi_1 = 0$, $\varphi_2 = \pi/2$, $\varphi_3 = \pi/8$, and $\varphi_4 = \pi/4$. Again, the analytical curve already agrees well with the empirical ones if only a low number of snapshots is available. Moreover, the empirical estimation errors of NC Standard ESPRIT and NC Unitary ESPRIT both using SLS match for a large sample size. The simulation results verify that the analytical expressions become exact as either the SNR or the number of snapshots becomes large.

6. CONCLUSION

In this paper, we have presented a first-order analytical performance analysis of 1-D NC Standard ESPRIT and 1-D NC Unitary ESPRIT both using SLS to solve the augmented shift invariance equation. We have derived a first-order approximation of the estimation error, which is asymptotic in the effective SNR and an explicit function of the noise perturbation, where no assumptions about the noise statistics are required. We have also found generic MSE expressions, that only assume the noise to be zero-mean and its SO moments to be finite. Furthermore, we have demonstrated via simulations that the empirical curves match the analytical ones and shown that the analytical performance of NC Standard ESPRIT and NC Unitary ESPRIT using SLS is the same in the high effective SNR. At low SNRs, however, NC Unitary ESPRIT with SLS performs better while requiring a lower complexity and should therefore be preferred in practice.

7. REFERENCES

[1] R. H. Roy and T. Kailath, "ESPRIT-estimation of signal parameters via rotational invariance techniques," *IEEE Transactions on Acoustics, Speech, and Signal Processing*, vol. 37, no. 7, pp. 984-995, July 1989.

[2] M. Haardt and J. A. Nossek, "Unitary ESPRIT: How to obtain increased estimation accuracy with a reduced computational burden," *IEEE Transactions on Signal Processing*, vol. 43, no. 5, pp. 1232-1242, May 1995.

[3] F. Li, H. Liu, and R. J. Vaccaro, "Performance analysis for DOA estimation algorithms: Unification, simplifications, and observations," in *IEEE Transactions on Aerospace and Electronic Systems*, vol. 29, no. 4, pp. 1170-1184, Oct. 1993.

[4] F. Roemer and M. Haardt, "A framework for the analytical performance assessment of matrix and tensor-based ESPRIT-type algorithms," arXiv:1209.3253, Sept. 2012.

[5] M. Haardt, "Structured least squares to improve the performance of ESPRIT-type algorithms," *IEEE Transactions on Signal Processing*, vol. 45, no. 3, pp. 792–799, Mar. 1997.

[6] F. Roemer and M. Haardt, "Analytical performance assessment of 1-D structured least squares, in *Proc. IEEE Int. Conf. Acoustics, Speech and Sig. Proc. (ICASSP)*, Prague, Czech Republic, May 2011.

[7] A. Zoubir, P. Chargé, and Y. Wang, "Non circular sources localization with ESPRIT," in *Proc. European Conference on Wireless Technology (ECWT 2003)*, Munich, Germany, Oct. 2003.

[8] M. Haardt and F. Roemer, "Enhancements of unitary ESPRIT for non-circular sources," in *Proc. IEEE Int. Conf. on Acoust., Speech, and Sig. Proc. (ICASSP)*, Montreal, Canada, May 2004.

[9] J. Steinwandt, F. Roemer, and M. Haardt, "Performance analysis of ESPRIT-type algorithms for non-circular sources," in *Proc. IEEE Int. Conf. on Acoust., Speech, and Sig. Proc. (ICASSP)*, Vancouver, Canada, May 2013.

[10] J. R. Magnus and H. Neudecker, *Matrix differential calculus with applications in statistics and econometrics*, John Wiley and Sons, 1995.

[11] F. Roemer and M. Haardt, "Deterministic Cramér-Rao bounds for strict sense non-circular sources," in *Proc. ITG/IEEE Workshop on Smart Antennas (WSA)*, Vienna, Austria, Feb. 2007.